Proceedings of the HS 2004, Smolenice castle, Slovakia

DIFFRACTION IN HIGH ENERGY *EP* COLLISIONS

ARMEN BUNYATYAN
Max-Planck-Institut für Kernphysik,
Saupfercheckweg 1, 69117 Heidelberg, Germany
and Yerevan Physics Institute, Armenia
E-mail: bunar@mail.desy.de

Representing the H1 and ZEUS Collaborations

Recent measurements of inclusive processes, vector meson production and hadronic final states in diffractive interactions at HERA are presented. The data are used to investigate the factorization properties and study the partonic structure of colour singlet exchange.

1 Introduction

In its first running period, which ended in 2000, the ep collider HERA delivered more than $100pb^{-1}$ of integrated luminosity for each of the two experiments H1 and ZEUS. In this report we present some recent results on diffractive physics.

The diffractive dissociation of the photon $\gamma p \to Xp$ has characteristics similar to diffractive hadron–hadron interactions and can be described by Regge phenomenology. Within this framework, diffractive interactions at high energies are dominated by the exchange of the Pomeron, an object with vacuum quantum numbers. On the other hand, perturbative QCD (pQCD) calculations can be made for diffractive processes in which a hard scale is present: processes with high virtuality Q^2 or high four-momentum transfer squared $|t|$, or processes where the high p_T jets or heavy quarks are produced. In pQCD, the vacuum exchange can be modelled as the exchange of a colour singlet gluon ladder between the proton and the virtual photon, which fluctuates into a $q\bar{q}$ or $q\bar{q}g$ state before the interaction [1]. In this approach, the cross section is factorized into the square of the effective dipole wave function and the square of the cross section for diffractive scattering of the dipole off the proton.

At HERA, it is possible to vary the scale with which the Pomeron structure is probed in diffractive interactions, to study its partonic content and the transition from soft to hard interactions.

2 Diffractive Vector Meson Production

Vector meson production has been extensively studied at HERA both in the photoproduction ($Q^2 \sim 0$) and DIS regimes ($Q^2 > 1\ GeV^2$). Fig.1a presents the exclusive photoproduction cross section for different vector mesons as a function of the γp center of mass energy, $W_{\gamma p}$ [2,3]. The cross sections for light vector mesons (ρ, ω, ϕ) follow the soft behaviour of the total photon–proton cross section parameterized as

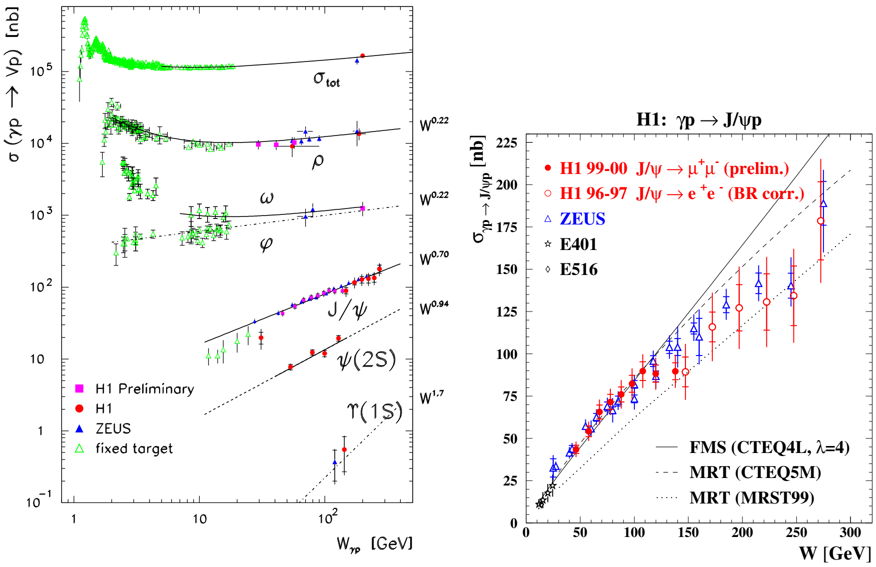

Figure 1. **a)** Vector meson cross sections as a function of the total CM energy of the photon-proton system $W_{\gamma p}$ in photoproduction ($Q^2 = 0$); **b)** The J/ψ meson cross section as a function of $W_{\gamma p}$ in photoproduction ($Q^2 = 0$) compared with pQCD calculations.

$\sim W^{0.2}$ in agreement with the predictions of the Regge approach [4]. In contrast, the J/ψ cross section exhibits much harder energy dependence ($\sim W^{0.8}$) [5,6]. Here, the mass of the charm quark sets the hard scale for pQCD calculations, and the steep energy dependence, which is related to the rise of the gluon density in the proton at small values of Bjorken-x, is quite well described by pQCD predictions [7] as seen in Fig.1b. In Fig.2a the J/ψ cross sections in photoproduction and in DIS regimes are compared with model predictions using different parameterizations of parton distribution functions (PDF) in the proton [8]. The data show a strong sensitivity to the choice of proton PDF.

Fig.2b shows the ρ cross section for different values of Q^2 as a function of W [9]. The energy dependence of the cross section becomes steeper as Q^2 increases. For light vector mesons, Q^2 plays the role of the hard scale, similar to the mass of the charm quark in the case of J/ψ photoproduction.

3 Deeply Virtual Photon Scattering (DVCS)

The Deeply Virtual Photon Scattering (DVCS) can be regarded as the elastic scattering of the virtual photon off the proton via a colourless exchange. The DVCS cross section depends on the generalized parton distributions (GPD), which carry information about the wave function of the proton. The simplicity of the final state and the absence of complications and uncertainties due to unknown vector meson wave function mean that the QCD predictions are more reliable than for many

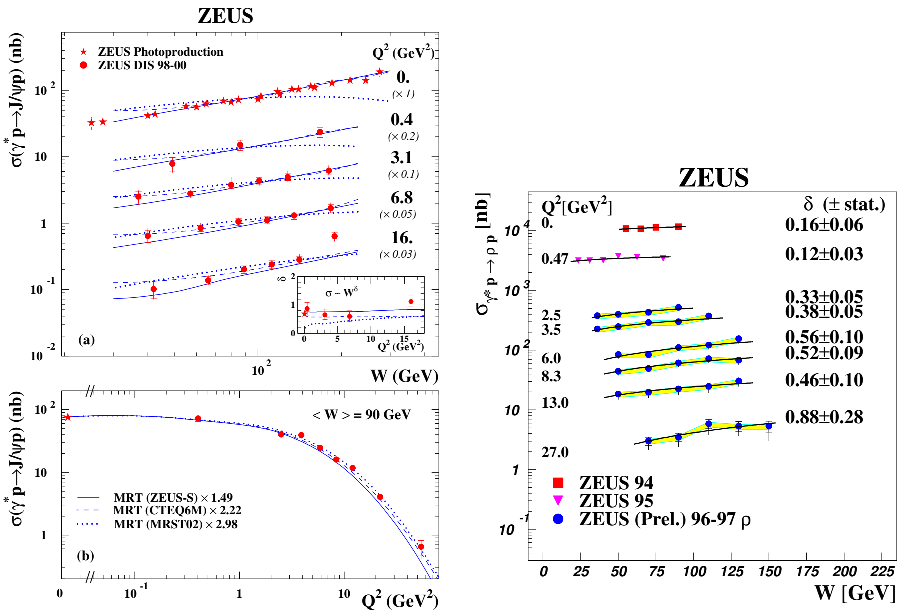

Figure 2. **a)** The J/ψ meson cross section as a function of W and Q^2 compared with pQCD calculations. **b)** The ρ meson cross section as function of W at different values of Q^2.

other exclusive final states.

The $\gamma^* p$ cross section for the DVCS process is shown in Fig.3 as functions of W and Q^2 [10,11]. The measurements are compared with the NLO QCD predictions based on different GPD parameterizations [12,13] and with the Colour Dipole model predictions [14]. The predictions are in good agreement with the measurements. The main difference between the results obtained from different parameterizations is a change of overall normalization due to the uncertainty in the t dependence.

4 Inclusive Diffraction in DIS

The kinematics of diffractive deep inelastic scattering, $ep \to eXp$, can be expressed in terms of the photon virtuality Q^2, the squared four momentum transfer t, Bjorken x, the fraction of the beam proton's momentum carried by the Pomeron, $x_{I\!P}$, and the fraction of the Pomeron's momentum carried by the struck quark, β. The cross section for the diffractive DIS process can be described by an expression analogous to that used for inclusive DIS:

$$\frac{d\sigma^D}{d\beta dQ^2 dx_{I\!P}} = \frac{2\pi\alpha}{\beta Q^4}(1 - y + \frac{y^2}{2})(F_2^D - \frac{y^2}{1+(1-y)^2}F_L^D)$$

In Fig.4 the new high precision H1 and ZEUS measurements of diffractive structure function are shown as a function of $x_{I\!P}$ for different Q^2 and β bins [15,16]. The

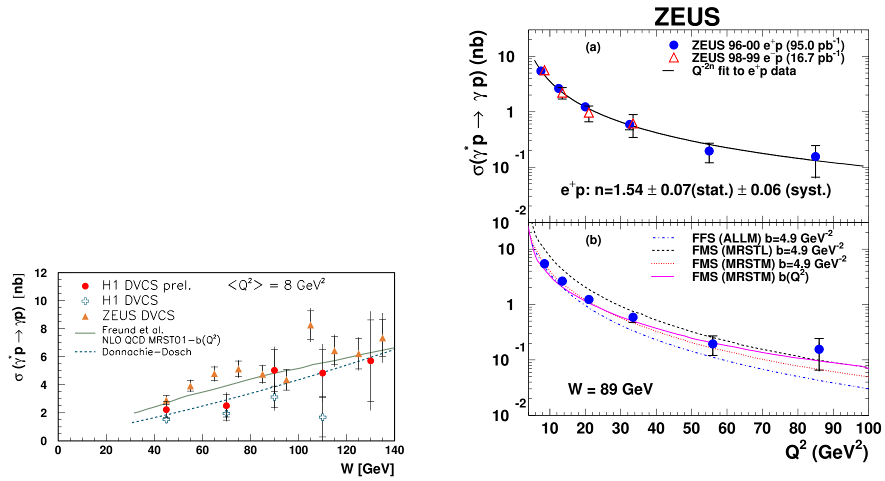

Figure 3. The $\gamma^* p \rightarrow \gamma p$ DVCS cross section as a function of W for $< Q^2 >= 8\ GeV^2$ and as a function of Q^2 for $W = 89\ GeV$. The GPD-based theoretical predictions are compared to the measurements.

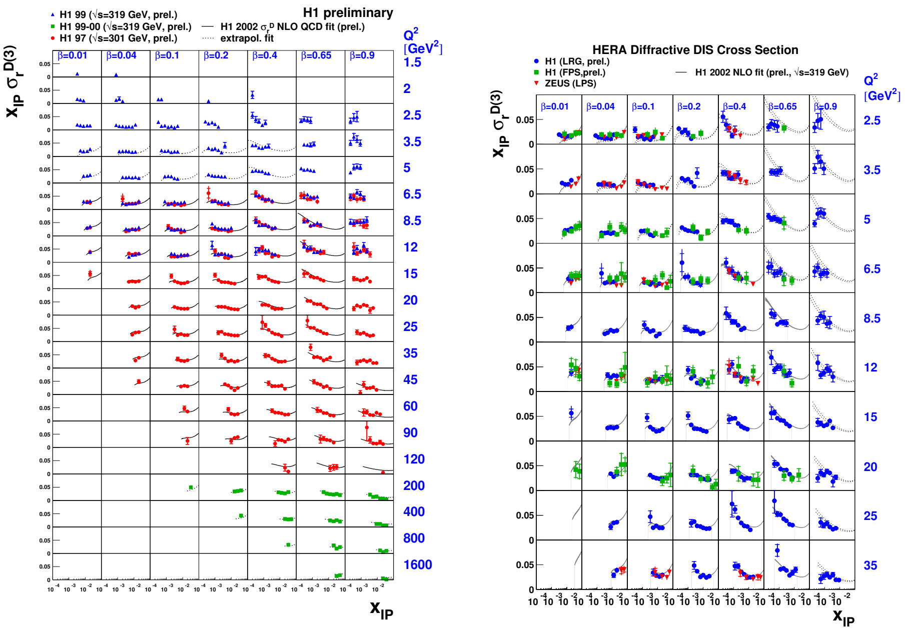

Figure 4. The reduced cross section $\sigma_R^D \equiv F_2^D - \frac{y^2}{1+(1-y)^2} F_L^D$ as a function of $x_{I\!P}$.

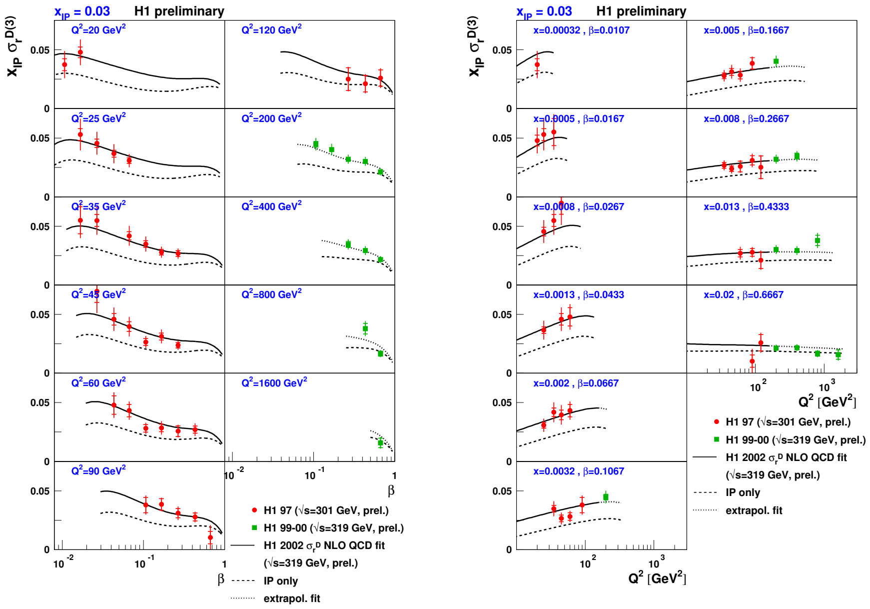

Figure 5. The reduced cross section $\sigma_R^D \equiv F_2^D - \frac{y^2}{1+(1-y)^2} F_L^D$ as a function of β and Q^2 for $x_{I\!P} = 0.03$.

measurements cover a large range of Q^2 between 1.5 and 1600 GeV^2. Fig.4 also demonstrates very good agreement between both H1 and ZEUS measurements.

The diffractive reduced cross sections $\sigma_R^D \equiv F_2^D - \frac{y^2}{1+(1-y)^2} F_L^D$ are shown in Fig.5 as functions of β and Q^2 for $x_{I\!P} = 0.03$. These plots indicate the different behaviour of diffractive and inclusive proton structure functions: the diffractive structure functions exhibit a relatively flat β dependence (β is analogous to x_{Bj} for the proton) and rising scaling violation up to relatively large values of β. These differences can be related to the very large gluon component in the diffractive processes.

These H1 measurements were used in a DGLAP QCD analysis in order to extract diffractive parton densities. The extracted NLO singlet quark $\Sigma(z, Q^2)$ and gluon densities $g(z, Q^2)$, together with their uncertainties, are shown in Fig.6 [17]. Here the variable z corresponds to the momentum fraction carried by an individual parton. The comparison of quark and gluon contributions shows that up to 75% of the Pomeron's momentum is carried by gluons. It is also apparent that due to the indirect extraction of $g(z, Q^2)$ from the scaling violation, the gluon densities at high z have large uncertainties.

5 Diffractive Dijet and Charm Production

According to the QCD factorization theorem [18], the parton distribution functions extracted from the QCD fits to diffractive structure functions can be used to

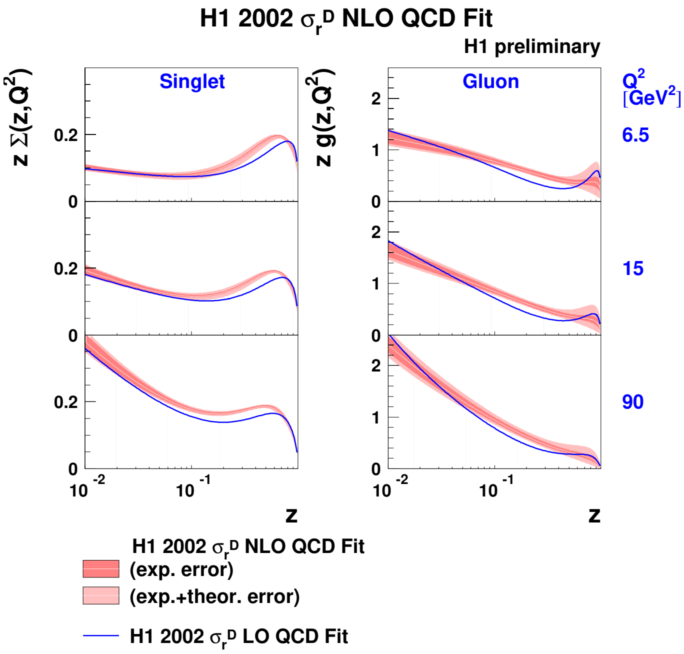

Figure 6. Pomeron parton densities. The left hand side shows the singlet quark distribution, the right hand side shows the gluon density.

describe hadronic final states in diffractive DIS. Of particular interest are measurements of open charm and diffractive dijet production since the boson–gluon fusion process provides a direct probe of the gluon content of the Pomeron, in contrast to inclusive measurements which are mainly sensitive to the quarks. The presence of a hard scale provided by the high transverse momentum of the jets or the mass of the charm quark allows the testing of different QCD based models.

The PDFs extracted from the LO and NLO QCD fits have been implemented in the DISENT [19] and HVQDIS [20] programs and used to make predictions for various hadronic final state observables [21].

Fig.7 shows the cross sections for diffractive D^* meson production in DIS as function of $p_T^{D^*}$ and β [22,23]. These measurements are compared with the RAPGAP Monte Carlo predictions [24] and with NLO calculations with HVQDIS [20] program which use 'H1 2002 fit' PDFs extracted from the fits to inclusive diffractive DIS data [17]. The NLO calculations, corrected for hadronization effects, provide within the theoretical and experimental uncertainties a reasonable description of the shape and normalization of the measured cross section. Fig.7 also demonstrates good agreement between the both experiments. The perturbative QCD calculations which use the unintegrated gluon density from CCFM evolution to the inclusive F_2 data [25] also provide a fair description of diffractive D^* data (not shown) [22]. The D^* results are thus consistent with QCD factorization in diffractive DIS.

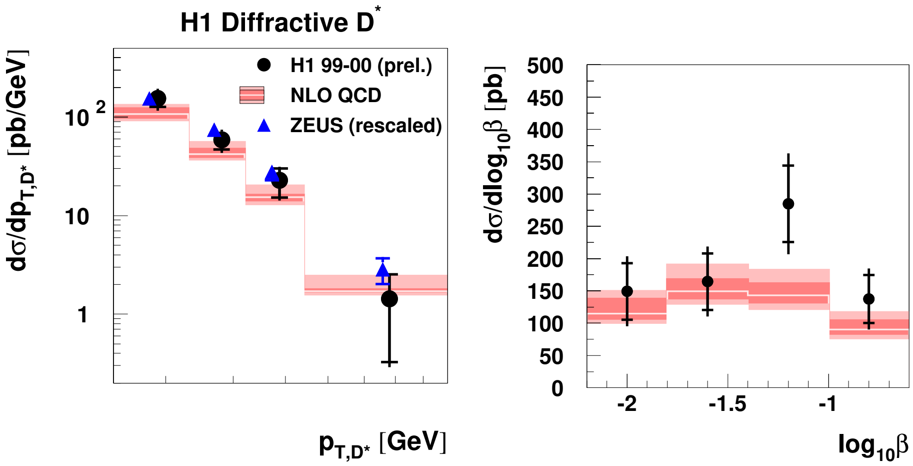

Figure 7. Cross section for the diffractive production of D^* in DIS. The HVQDIS prediction based on the 'H1 2002 fit' diffractive PDFs at NLO are compared with the measurements.

Dijet production in diffractive interactions was studied in the DIS and photoproduction regime [26,27]. In the photoproduction, the resolved and direct processes are distinguished by reconstructing the variable x_γ, defined as the fractional momentum of the quasi-real photon entering the dijet system. For direct processes $x_\gamma = 1$, while in the case of resolved processes $x_\gamma < 1$ will hold.

Fig.8 displays the measured cross sections for diffractive dijet in DIS together with the predictions of RAPGAP Monte Carlo and the DISENT NLO calculations [19]. The 'H1 2002 NLO' fit to inclusive DIS data was used for diffractive PDFs. The NLO predictions corrected for hadronization provide a good description of the measurement, supporting the QCD factorization in diffractive DIS.

The conclusion is however different in case of photoproduction. Fig.9 displays the measured cross sections for diffractive dijet photoproduction together with the prediction of NLO program of Frixione et al. [28]. In contrast to the DIS case, here the NLO predictions overestimate the cross sections by about a factor 2. The NLO predictions describe the cross sections within the errors if the additional scaling factor of 0.5 is applied to both the resolved and direct components, thus indicating the breakdown of the QCD factorization in diffractive photoproduction.

It is interesting to note that the diffractive dijet analysis made by CDF Collaboration in the process $p\bar{p} \to pX$ at $\sqrt{s} = 1800\ GeV$ [29,16] shows larger discrepancy between the predictions based on 'H1 2002 fit' PDFs and their measurements. This breakdown of factorization has often been interpreted as being due to additional spectator interactions which lead to the suppression of the diffractive cross section. It was suggested [30] that due to such spectator interactions for diffractive photoproduction of jets the resolved component has to be suppressed by a factor ~ 0.34. However the suppression of only resolved component as predicted by theory is not supported by H1 and ZEUS measurements.

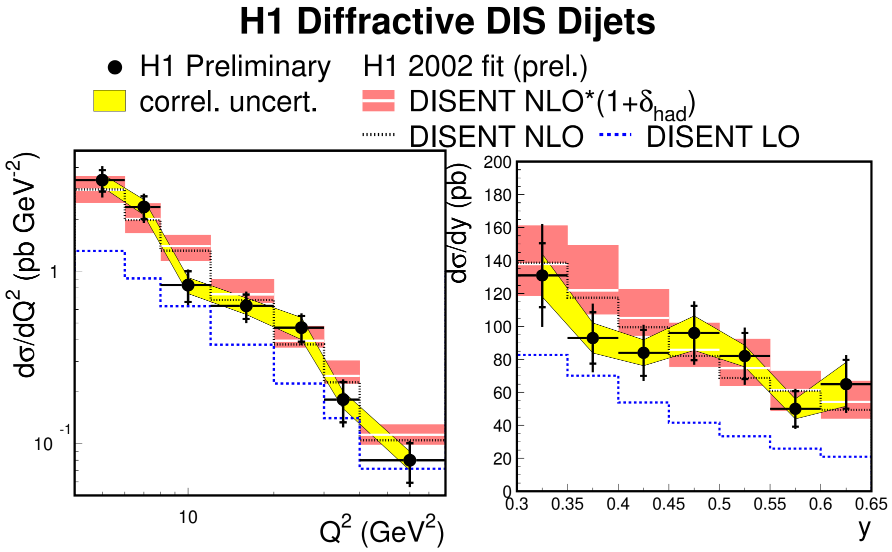

Figure 8. Cross section for the diffractive production of two jets in DIS. The DISENT prediction based on the 'H1 2002 fit' diffractive PDFs at NLO are compared with the measurements.

6 Dijets and Charm Production with Leading Neutrons

In analogy to diffractive processes, the factorization can be further tested in dijet and open charm events with a leading neutron in the final state. The dominant mechanism for leading neutron production is the exchange of π^+-meson [31]. The left hand side plot in Fig.10 shows the ratios of leading neutron tagged D^* meson production to to the total D^* production in photoproduction [32]. These ratios are almost flat for all variables - W, p_T and η. The right hand side plots in Fig.10 shows the similar ratios for dijet events [33]. The data show no significant dependence on E_T^{jet} and Q^2, in agreement with the hypothesis of vertex factorization.

7 Conclusions

HERA is an ideal facility for the study of the transition from soft to hard diffraction, explored using different hard scales $(Q^2, M_q, p_T^{jet}, ...)$.

The measurements of inclusive diffraction and the hadronic final state in diffractive DIS can be described within a consistent picture. The results support QCD factorization with diffractive parton densities which are evolved according to the DGLAP equations and are dominated by the gluon contribution.

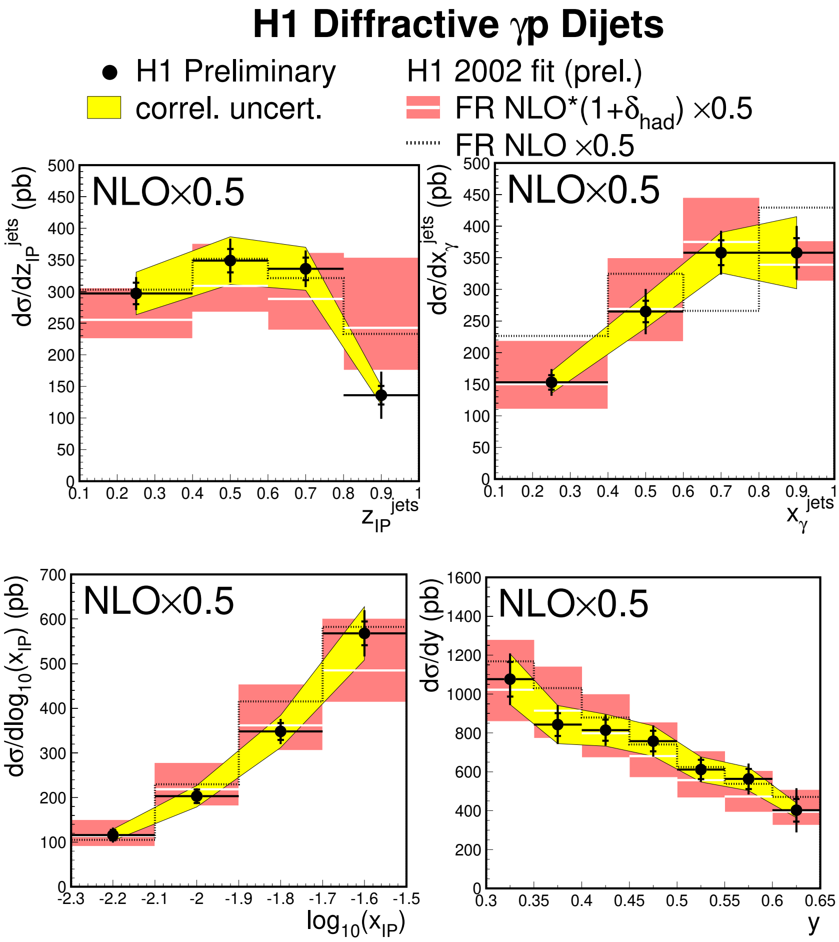

Figure 9. Cross section for the diffractive production of two jets in photoproduction. The prediction of NLO program of Frixione et al. [28] interfaced with the 'H1 2002 fit' diffractive PDFs at NLO and scaled by a factor 0.5 are compared with the measurements.

Acknowledgements

I would like to thank organizers for this interesting, stimulating and enjoyable conference.

References

1. For a review see M. McDermott, DESY 00-126 (2000).
2. H1 Collaboration, *Nucl. Phys.* **B 463** (1996) 3; *Phys. Lett.* **B 541** (2002) 251.

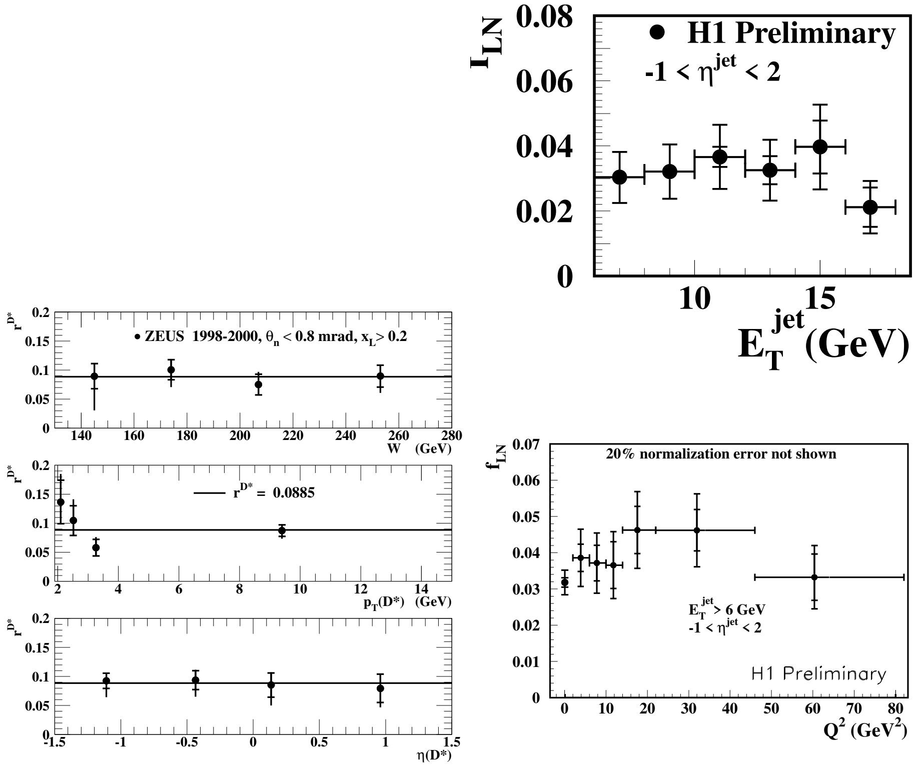

Figure 10. **(left)** The ratio of neutron-tagged D^* production to the total D^* sample as a function of W, $p_T(D^*)$ and $\eta(D^*)$. **(right)** The ratio of neutron-tagged dijet production to the total dijet samples a function of E_T^{jet} in photoproduction and as a function of Q^2.

3. ZEUS Collaboration, *Phys. Lett.* **B 377** (1996) 259; *Z. Phys.* **C 73** (1996) 73; *Eur. Phys. J.* **C 2** (1998) 247; *Phys. Lett.* **B 437** (1998) 432.
4. A. Donnachie and P. Landshoff, *Phys. Lett.* **B 296** (1992) 227.
5. H1 Collaboration, contributed paper 108 to EPS03, Aachen.
6. ZEUS Collaboration, *Eur. Phys. J.* **C 24** (2002) 345; *Phys. Lett.* **B 437** (1998) 432.
7. A.D. Martin, M.G. Ryskin and T. Teubner, *Phys. Rev.* **D 62** (2000) 14022; L. Frankfurt, M. McDermott and M. Strikman, *Journal High Energy Phys.* **103** (2001) 45.
8. ZEUS Collaboration, *Nucl. Phys.* **B 695** (2004) 3.
9. ZEUS Collaboration, contributed paper 594 to EPS2001, Budapest.
10. ZEUS Collaboration, *Phys. Lett.* **B 573** (2003) 46.
11. H1 Collaboration, Abstract 6-0182, 32nd International Conference on High Energy Physics, Beijing, China, 2004.
12. A. Freund and M.F. McDermott, *Eur. Phys. J.* **C 23** (2002) 651.
13. L. Frankfurt, A. Freund and M. Strikman, *Phys. Lett.* **B 460** (1999) 417651.

14. A. Donnachie and H.G. Dosch, *Phys. Lett.* **B 502** (2001) 74.
15. ZEUS Collaboration, contributed paper 538 to EPS03, Aachen.
16. H1 Collaboration, Abstract 6-0175, 32nd International Conference on High Energy Physics, Beijing, China, 2004.
17. H1 Collaboration, contributed paper 089 to EPS03, Aachen.
18. J.C. Collins, *Phys. Rev.* **D 57** (1998) 3051; *Phys. Rev.* **D 61** (2000) 019902.
19. S. Catani, M.H. Seymour, *Nucl. Phys.* **B 485** (1997) 29;
F. Hautmann, *Journal High Energy Phys.* **210** (2002) 25.
20. B.W. Harris, J. Smith, *Phys. Rev.* **D 57** (1998) 2806;
L. Alvero, J.C. Collins, J.J. Whitmore, hep-ph/9806340.
21. H1 Collaboration, Abstract 6-0176, 32nd International Conference on High Energy Physics, Beijing, China, 2004.
22. H1 Collaboration, Abstract 6-0178, 32nd International Conference on High Energy Physics, Beijing, China, 2004.
23. ZEUS Collaboration, *Phys. Lett.* **B 545** (2002) 244.
24. H. Jung, *Comp. Phys. Commun.* **86** (1995) 147.
25. J. Bartels, H. Jung and A. Kyrieleis, *Eur. Phys. J.* **C 24** (2002) 555;
J. Bartels, H. Jung and M. Wüsthoff, *Eur. Phys. J.* **C 11** (1999) 111.
26. H1 Collaboration, Abstract 6-0177, 32nd International Conference on High Energy Physics, Beijing, China, 2004.
27. ZEUS Collaboration, Abstract 6-0249, 32nd International Conference on High Energy Physics, Beijing, China, 2004.
28. S. Frixione, Z. Kunszt and A. Signer, *Nucl. Phys.* **B 467** (1996) 399;
S. Frixione, *Nucl. Phys.* **B 507** (1997) 295.
29. CDF Collaboration, *Phys. Rev. Lett.* **84** (2000) 5043.
30. A. Kaidalov et al., *Phys. Lett.* **B 567** (2003) 61.
31. J.D. Sullivan, *Phys. Rev.* **D 5** (1972) 1732;
H. Holtmann *et al.*, *Phys. Lett.* **B 338** (1994) 363;
B. Kopeliovich, B. Povh and I. Potashnikova, *Z. Phys.* **C 73** (1996) 125.
32. ZEUS Collaboration, Abstract 6-0324, 32nd International Conference on High Energy Physics, Beijing, China, 2004.
33. H1 Collaboration, Abstract 6-0763, 32nd International Conference on High Energy Physics, Beijing, China, 2004.